For all tanks prone to store energy

Alfredo Angelillo[1], Walter Gaggioli[2], Primo Di Ascenzi[2], Valeria Russo[2]

[1] REEFS2, Oslo (Norway)

[2] ENEA Italian National Agency for New Technologies, Energy and Sustainable Economic Development, Casaccia-Rome (Italy)

Abstract

Two decades' data analysis from a molten salt fully instrumented tank has led to significant advancements in methodologies and a deeper understanding of key phenomena related to molten salt energy storage. This includes new insights into the natural temperature decay of molten salt for the significant high melting point. The developed analytical solution for determining the thermal displacement of inertia phase provides evidence of a distinct core and the internal physical relationships of the tank. Controlling this phenomenon is essential for predicting and defining storage tank performance over time by optimally utilizing the thermal inertia of the molten salt core, and it serves as a start point for both on-design modelling—optimal tank geometries and their components to ensure durability under specified operating conditions—and off-design scenarios, where predetermined geometries and boundary conditions allow for computation of operational parameters for an improved storage tanks, its internal heat exchanger or insulation ageing prediction. The presented analytical solution demonstrates strong correlation with empirical observations and introduces improved control via the Navier-Stokes-Fourier equations and Law of the Wall. Additionally, the study proposes reliable simplifications through a lumped-circuit approach, drawing a novel analogy to a junction diode for wall and skin condition analyses. A coupled fluid dynamic solution employing the Lewis number further enhances the accuracy of computations based on the physical properties of the control volumes.

Keywords: Storage, Performance, Lumped Circuit, Lewis Number, Navier-Stokes-Fourier, Law of wall, CSP

1. Introduction

Natural temperature decay behaviours about skin effects have been observed in about 20 years of continuous operation data on a single and the same fully instrumented tank for the NaNO3-KNO3(60-40) mixture (Janz et al.,1968; Janz and Bansai, 1982). The identification of an ideal initial condition at the installed year of ENEA research Centre's test station, i.e. between 9.7.2004 and 12.7.2004, independent of other collateral phenomena, has allowed to correctly model the temperature trends in the four conditions in which the thermocouples were installed: immersed in the molten salts; between the molten salts and ullage; in the ullage; and, on the shell of the tank. As matter of fact, three internal trend conditions can always be identified, namely molten salt, interface between molten salt and ullage, and only ullage, see Figure 3. While the last two can be closely related to how natural decay occurs according to transient conduction (Bergman and Lavine, 2017), the molten salt does not. De facto, an accurate assessment of the operational trend with particular attention to the effects of observed pressure and temperature variations on the physical properties of fluids has been conducted. Specifically, and in regard of this analysis, the base parameters have been identified for all the conditions in which the tank operates at atmospheric pressure or below $1.5*10^5$ Pa and at temperatures between 240°C and 550°C. These two boundary parameters are decisive in establishing the physical-operational state of the molten salt mass in a diathermic system during the natural decay, affecting factors such as compressibility. This directly reflects in the efficiency of storage systems: detailed knowledge of the energy level trend and its relative compressibility. Data analysis shows that, in no stationary states for the mass of molten salts, an increase in pressure leads to a rise in energy level; however, beyond a certain threshold, i.e. more than $1.5*10^5$ Pa, the compressibility of the fluid increases considerably.

Furthermore, thorough analysis of independent variables — velocity, position, time, and temperature — enables precise description of the system state in various operating scenarios, providing a solid foundation for

10.18086/swc.2025.01.09 Available at http://proceedings.ises.org

advanced control and monitoring strategies. It is particularly relevant, for example, to consider the rapidity of heat transfer from the piping tracings to the salt mass in the tank: this process, depending on the plant layout, occurs instantaneously via steel piping; and this obviously leads to erroneous data interpretations.

Briefly, the analytical solution and verification with both experimental and historical real data contribute to improving the reliability of measurements and the management of thermal and mechanical transitions within the tanks. One practical example is the geometric definition of a molten salt core characterized by variable thermal inertia, as a function of the design or existing configuration, which enables optimization of the placement of inlets, outlets, or any heat exchangers inside the tanks. Since 2004 the existence of a core in the molten salt mass with higher thermal inertia compared to the decay conditions formulated in literature has always been observable. As matter of fact, the exanimated tank with a minimum mass of 2.4 m³ molten salt shows the stratified current flows towards the exterior tank-skin with a thermal inertia of about ten hours before naturally decay. Furthermore, it has been possible to assess the performance trend over time in relation to the state of thermal insulation, allowing for the development of a method to predict targeted maintenance interventions aimed at energy optimization; this aspect and related automation are further explored in a study currently being published. Therefore, this paper focuses mostly on the algorithm to estimate thermal displacement associated with the inertial boundary layer, beginning with the general conditions for thermodynamic balance and equilibrium. Indeed, a combined modelling of the reference masses, molten salts, and ullage, according to the Navier-Stokes approach, integrated with the indications from Fourier's postulate (Chaudhuri and Feireisl, 2022) as well as the knowledge of the independent variables — velocity, position, time, and temperature — has therefore formed the basis for defining the wall boundary conditions. The solution through the law of the wall and the GRG method for calculating the limit values combined with the thermal displacement have provided the necessary inputs for determining the inertia of the molten salt core. As a result, this was associated with the skin effect as a diode-junction, within lumped-circuit representation, for subsequent simulation both in OpenFoam as visual one and in OpenModelica as the simplest and most effective tool for finding the necessary solutions to the fundamental equations for convective dynamics of the ullage versus molten salt volume, which will be detailed in a forthcoming publication.

2. Methodology

The analysis carried out, while considering a variety of scenarios and broader operating conditions, focuses on a well-defined set of parameters that outline its field of application and ensure its consistency. Specifically, the fundamental validity conditions are pressure, temperature, and physical state. The tank operates at atmospheric pressure or, in any case, at values not exceeding $1.5*10^5$ Pa in accordance with selected data. This range represents the upper limit beyond which the compressibility of molten salts increases significantly, making the Newtonian modelling no longer suitable and introducing non-negligible effects on the dynamics of the non-adiabatic system. In particular, for pressures above the validity range, the compression of the salt fluid amounts to 1.2÷1.8 mm kPa^{-1}. The temperature range taken into account goes from 240°C to 550°C. This range encompasses the actual operating conditions typical of thermal storage systems based on NaNO3-KNO3 60/40 allowing assessment of changes in energy level and the physical properties of the fluid in relation to thermal fluctuations. The physical and operational conditions resulting from the temperature and pressure described define the state of the controlled volumes, its boundary conditions, and the incompressibility of the heat storage fluid as well as the thermodynamic behaviour of the entire tank system.

In summary, compliance with these parameters forms the methodological basis on which the reliability of the analyses derived from real data is established, ensuring that the conclusions and predictions obtained are truly representative of the real trends of the system under examination. Given that the density ρ, specific heat c_p, dynamic viscosity μ and thermal conductivity k can be written as function of temperature T, and temperature and velocity $\tilde{u}$ are function of position and time (x_i, τ), experimental literature data on molten salts make it so that the laws governing the variation of dependent and independent variables can be represented as n-tuples:

$$\forall(x_i,\tau)\ \exists\{\tilde{u},T\}\colon\{u_i,T\} \rightarrow \{\rho,\mu,k,c_p\} \qquad \text{(eq. 1)}$$

The NaNO3-KNO3 60/40 experimental data from the literature have been reported in the captions of the figures 1 and 2. This means that the functions of physical quantities have been subjected to constrain based on the distribution of the data points and in order to remain within a physical range of validity that indirectly

considers an unavoidable measurement error.

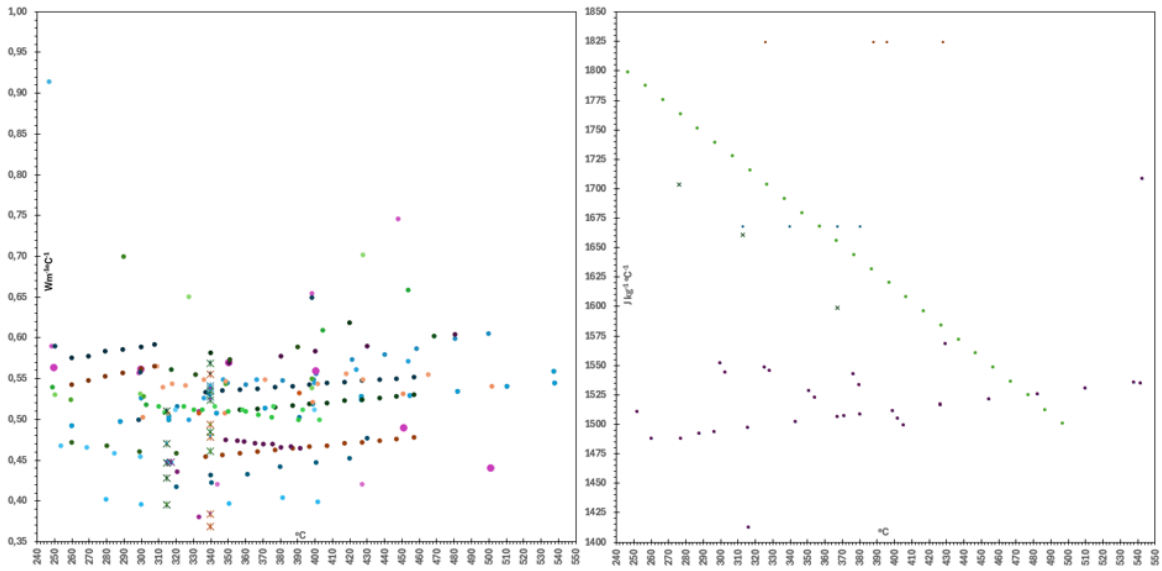

Figure 1:

Left side is the overlap conductivity [W m^{-1} $°C^{-1}$] data measures by [°C] (Zavoico, 2001), (Milozzi et al. 2001), (K. Cornwell, 1970), (Bradshaw and Carling, 1987), (Janz et al., 1979), (Anagnostopoulos et al., 2019), (Nunes et al., 2016), (Bonk and Bauer, 2021), (Qing-Guo Zhao et al., 2017), (Afrah Awad et al., 2018), (Ze Sun et al. 2021), (Saivenkataraman et al., 2010), (Zhang and Fujii, 2000), (DiGiulio and Teja, 1992)
Right side is the overlap specific heat [J kg^{-1} $°C^{-1}$] data measures by [°C] (Zavoico, 2001), (Milozzi et al. 2001), (Bradshaw and Carling, 1987), (Janz et al., 1979), (Nunes et al., 2016)

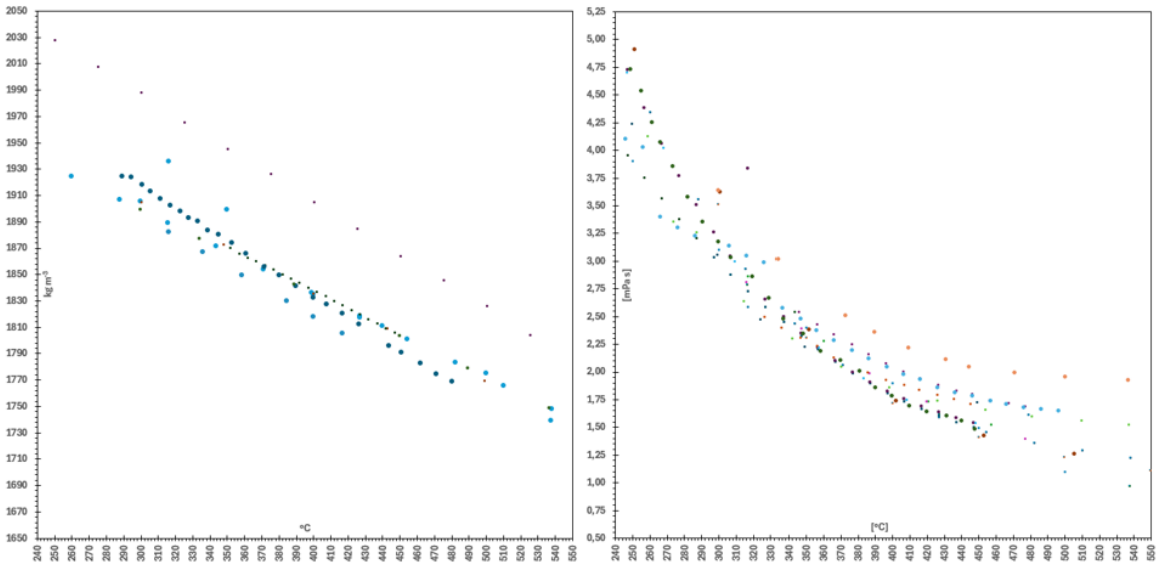

Figure 2

Left side is the overlap density [kg m^{-3}] data measures by [°C] (Zavoico, 2001), (Milozzi et al. 2001), (Bradshaw and Carling, 1987), (Janz et al., 1979), (Anagnostopoulos et al., 2019), (Nunes et al., 2016)

Right side is the overlap dynamic viscosity [mPa s] data measures by [°C] (Zavoico, 2001), (Milozzi et al. 2001), (Bradshaw and Carling, 1987), (Janz et al., 1979), (Anagnostopoulos et al., 2019), (Nunes et al., 2016), (Bonk and Bauer, 2021), (Ze Sun et al. 2024), (Saivenkataraman et al., 2010)

3. Model equations

The primary purpose of defining the modelling equations is to find the inertial thermal phase displacement of thermocouples immersed in molten salts that do not immediately follow the decay according to a law of conduction transients. This implies, starting from the first law of thermodynamics, that the conservation of

energy at any instant takes into account the reversible and irreversible losses of the energy balance. That is, starting from the most general relationship, the balance between stored, inlet and outlet energy plus that which is generated should be equalized. This equilibrium must be consistent with the number of variables and equations needed to find the solution. First, one can characterize with respect to the heat flow interested in, obtaining the general relationship in accordance with transient heat transport, where neglecting the heat transfer by radiation, two balance equations are obtained if applied separately to the ullage and to the molten salts' masses, and where their sum must equal the initial state:

$$q''_s A_{s,cond} - q''_{conv}\, A_{s(c,r)}\big|_{ull} = \rho V c_p \frac{\partial T}{\partial \tau}\Big|_{ull} \qquad \text{(eq. 2)}$$

$$q''_s A_{s,cond} + \dot{E}_g - q''_{conv}\, A_{s(c,r)}\big|_{ms} = \rho V c_p \frac{\partial T}{\partial \tau}\Big|_{ms} \qquad \text{(eq. 3)}$$

where for the ullage Nu >>1 at the operating temperatures, i.e. thermal conduction is negligible. In particular, for the sake of simplicity, the repetition of convection coefficient h, mass m, area or surface A and volume V, as well as time constant τ_T have been compacted according to the following notations:

$$\begin{aligned} &\theta = T - T_\infty \rightarrow d\theta = dT \\ &\theta_i = T_i - T_\infty \rightarrow d\theta_i = 0 \\ &b = \frac{hA}{m c_p} = \frac{hA}{\rho V c_p} = \tau_T^{-1} \\ &a = \frac{1}{m c_p} \end{aligned} \qquad \text{(eq. 4)}$$

Therefore, considering the problem only with regard to the molten salt heat loss as if it were wrapped in that of the air, under the hypothesis that the thin layer of steel delineates this mass, it follows that one can neglect what is due to conduction and the only meaningful equation between ullage and molten salt becomes the following, given $\dot{E}_g$ as initial generated energy and $\dot{E}_{st}$ as stored energy in whole tank system:

$$\begin{aligned} &\dot{E}_g - hA\theta = \frac{1}{a}\frac{\partial \theta}{\partial \tau} = \dot{E}_{st} \\ &\dot{E}_g = \dot{Q}_0(\theta, \tau) \end{aligned} \qquad \text{(eq. 5)}$$

However, to solve the equation in order to know the natural decay of temperatures and subjects to the constraints, the most general form of equation that governs the decay of temperatures, with or without initial inertial energy, will be of the form:

$$\theta = \theta_i e^{-b\tau} + \frac{a}{b}\dot{P}(\theta, \tau) \qquad \text{(eq. 6)}$$

Where P-equation is the part that strongly depends on the boundary conditions and which in any case will never equal the decay of the molten salts precisely because of the existence of the inertial phase displacement possessed by salt for any condition. Indeed, the error for the molten salts will be as large as the distance from the onset initial temperature is. The analysis leads to the differentiation of three types of readings: molten salt; molten salt-ullage interface; and ullage. In the latter two cases, the heat loss during decay coincides perfectly with that of the thermal conduction transient. The graph in Figure 3 sums up the energy injection phase and the decay phase depending on the thermocouple location, and the correspondence with the classical conduction transient law. The trend of the molten salt thermal lag (called also displacement) of inertial phase φ as a function of the height variation was first approximated to a parabolic equation and the heat exchange according to a logarithmic function. In essence, the closer the level of salts taken into consideration to the ullage (the thermocouple that measures it) the more the inertial phenomenon is reduced. This core challenges the known temperature decay trend due to a time lag, behaving like an inertial heat exchanger. Its fluid-dynamic trend leads to considering the heat transport gradient as a function of the velocity, which tends to zero as a given condition approach. Therefore, the Navier-Stokes equations, formulated with the appropriate boundary conditions, allow to find the temperatures and velocities towards the skin conditions. Specifically, the problem is solved by calculating the heat balance between two fluid dynamic conditions: one for ullage and the other for molten salts. For the Navier-Stokes thermodynamic equilibrium equation, an important observation must be made regarding the term derived from the Fourier Postulate, namely the diffusion of heat in a generally solid, homogeneous, and isotropic medium.

Although extensively verified, the postulate has two peculiarities: it is a so-called parabolic equation, which justifies internal conduction within salts; it also predicts infinite propagation for thermal perturbations, and it

loses validity in the case of very high gradients and very short times. In particular, considering a nearly constant volume, with approximately constant density, the physical principle of heat flow can be written independently of the causes or mechanism of heat transport itself. If it is possible to approximate the internal energy U to a solid state of the mass of salts with natural temperature decay then it can formulate the so-called Fourier Equation, if and only if one can write the variation of internal energy U as in a solid state and only dependent on the specific heat regardless of whether at constant volume or pressure. By setting the three equilibria (mass, dynamics and thermodynamics) of the Navier Stokes equations and starting from their convective notation, the general expressions to characterize according to section 4. Boundary conditions are:

$$\frac{D\rho}{D\tau} = -\rho \frac{\partial u_i}{\partial x_i} \qquad \text{(eq.7)}$$

$$\rho \frac{D\tilde{u}}{D\tau} = -\nabla p + \nabla \hat{d} + \rho \tilde{g} \qquad \text{(eq. 8)}$$

$$\rho \frac{De}{D\tau} = -p\nabla\tilde{u} + \nabla \cdot (k\nabla T) + \hat{d}\nabla\tilde{u} \qquad \text{(eq. 9)}$$

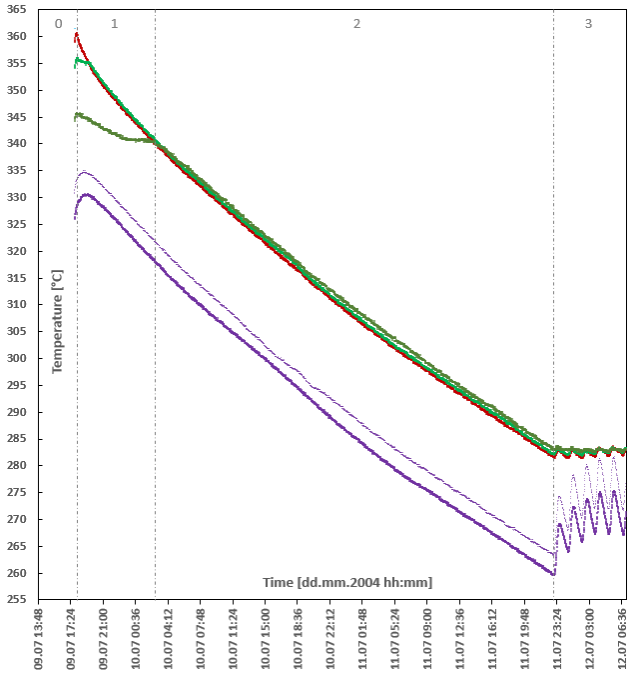

Figure 3 The reference dates in 2004 show typical conditions for thermocouple decay in 3 days. The thermocouples in the ullage are purple, the ullage-molten salt interface is red, and those immersed in the molten salts are green. At the top, the one closest to the ullage-molten salt interface is light green (1,5-hour displacement), while the one closest to the core of the mass is dark green, with an inertia of approximately 10 hours. The 0-zone is the end of supplied energy to tank. The 1-zone is the thermal inertia phase of molten salt. The 2-zone is a stratified natural decay according to transient conduction. The 3-zone is the backup-phase.

Furthermore, the thermodynamic equations of entropy, enthalpy and temperature using the material derivative were helpful in analytical verification once the boundary conditions were applied.

$$\rho T \frac{Ds}{D\tau} = \rho \frac{De}{D\tau} - \frac{p}{\rho}\frac{D\rho}{D\tau} = \nabla \cdot (k\nabla T) + \hat{d}\nabla\tilde{u} \qquad \text{(eq. 10)}$$

$$\rho \frac{Dh}{D\tau} = \rho T \frac{Ds}{D\tau} + \frac{Dp}{D\tau} = \frac{Dp}{D\tau} + \nabla \cdot (k\nabla T) + \hat{d}\nabla\tilde{u} \qquad \text{(eq. 11)}$$

$$\rho c_p \frac{DT}{D\tau} = \beta T \frac{Dp}{D\tau} + \nabla \cdot (k\nabla T) + \hat{d}\nabla\tilde{u} \qquad \text{(eq. 12)}$$

The problem posed thus far may be undefined, as the Navier-Stokes equations do not intrinsically express when the inertial phenomenon ends. Therefore, to determine the conditions of time and space under which velocity approaches zero, it is necessary to assess the thermal inertial phase delay of molten salt. Furthermore, an as yet unresolved condition arises: the general hypothesis of the Fourier postulate, involving an infinite or independent gradient of heat transport, contradicts the wall conditions, i.e., the Law of Wall, where the velocity tends to zero in a significant thickness between the tank skin plate and the layer of salts bordering it. This argument, of course, does not apply to air, where convection is assumed to be the primary heat transport, hence

conduction in the ullage is negligible. Here, the observation comes in that by letting the dimensionless velocity tend to zero while maintaining the Fourier postulate, the problem is solved, and the limiting thickness for which the inertial phase lag of the heat flow occurs according to the currents of the mass of salts is found. Or in other words, the process that identifies when and how long the thermal phase displacement will occur is connected to the trend of the wall conditions tending to zero; that is, the velocity gradient serves to find the point in the boundary layer at which the inertial phase lag ends in time. It follows that it is necessary to find the two fundamental values of the law of the wall, see Figure 4.

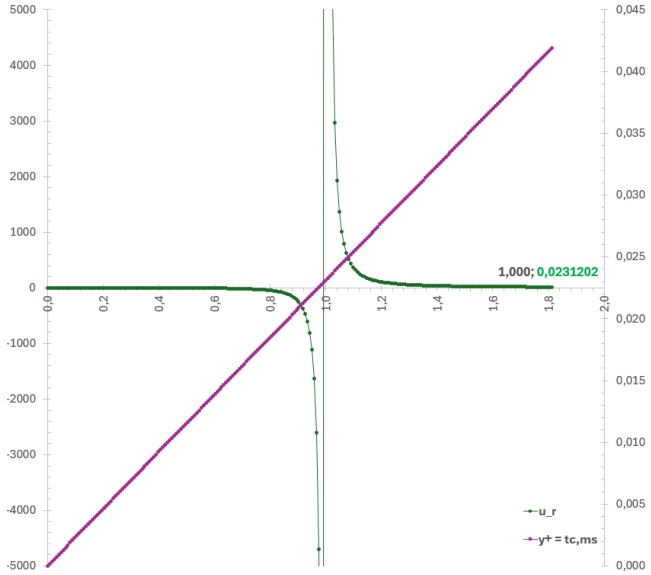

Figure 4 Shear velocity and dimensionless y^+ in the collapse phase. The x-axe is the dimensionless y^+. Left y-axe is the shear velocity u_r. The right y-axe is the thermal limit y [m]. The green value is the searched the thermal boundary layer of inertia lag.

Recalling the general expression of law of the wall:

$$u^+ = \begin{cases} \frac{1}{\kappa} ln\, y^+ + B \\ y^+, near\ to\ wall \end{cases} \qquad \text{(eq. 13)}$$

also:

$$\begin{cases} u^+ = \frac{u}{u_r} = \frac{u}{\sqrt{\frac{\tau_w}{\rho}}} \\ y^+ = \frac{y}{y_0} = \frac{y u_r \rho}{\mu} \end{cases} \qquad \text{(eq. 14)}$$

Where the shear velocity depends on the shear stress. According to Sau et al. (2013), shear stress is expressed as the shear rate where the velocity is related to the distance between ideal parallel sliding planes. Particularly, Sau et al. (2013) experimentally demonstrates that there is a linearity of the shear stress for molten salts and the possibility of considering molten salts as a Newtonian fluid within the temperature range of this study. Therefore, known the value of shear stress as a function of the salt temperatures, one can define the dimensionless value of the velocity. Regarding the Von Karman constant κ, a value of 0.40 is used, and for experimentally defined values between 0.35 and 0.42, no appreciable differences occur in the matter of this paper. Finally, the fluid dynamic coefficient B is set to 0 since, as a good approximation, it is not significant transient or turbulent fluid conditions. Hence, the fundamental equation for dimensionless velocity becomes:

$$u^+ = \frac{1}{\kappa} ln\, y^+ = \frac{1}{\kappa} ln\left(\frac{y u_r \rho}{\mu}\right) \qquad \text{(eq. 15)}$$

And the solution is found if and only if $u^+ \to 0$ which implies that $y^+ = \frac{y u_r \rho}{\mu} \to 1$ and infinite shear velocity. Having set up the problem in this way, the objective is to find the value that minimizes $u^+ \to 0$ by modifying the value of y. In these circumstances, the Generalized Reduced Gradient Method (GRGM) is suitable to obtain $y = \delta_t$. Along data analysis, the thermal phase lag has been found strongly connected to the Law of the wall and therefore once the thermal boundary layer is calculated, it follows by definition that:

$$\delta_t = \sqrt{\frac{k\tau_P}{c_p\rho\pi}} = \sqrt{\frac{\alpha\tau_P}{\pi}} = \frac{\sqrt{\alpha\varphi}}{\pi} \quad \text{(eq. 16)}$$

Where the inertial thermal displacement or lag is:

$$\varphi = \frac{\delta_t^2\pi^2}{\alpha} \quad \text{(eq. 17)}$$

which closes the algorithm by starting again with a further layer of molten salts as a function of the height.

4. Boundary conditions

The modelling equations presented in the previous section have been solved by assuming the following steps to characterize them.

Firstly, the thermal equilibrium between ullage and molten salts described in (eq. 2) and (eq. 3) plus (eq. 5) or (eq. 6) does not require an additional interface equilibrium within the context of this paper for two main reasons. The first is that, once internal energy generation stops, the decay phase begins simultaneously for both media; no transients or faster temperature gradients toward external conditions are present. This is supported by a comparison between internal and skin thermocouple readings: the temperature gradients measured at the same layer, or tank height, are parallel for the inertial phenomenon described here, indicating that the steel of the tank responds directly to the internal conditions just with a lower temperature. This suggests that the heat capacity at the interface between the two media can be considered quasi-adiabatic. Particularly, the relationship between ullage and molten salts led to the consideration of the Lewis number, even in the absence of a substantial mass transfer, with the aim of finding the value of the convection coefficient to be used and recalling the hypothesis that the value of *n* for Le is used to be 1/3. From the mass-transfer fluid laws and Fick's law it can be calculated the convection mass transfer coefficient, given a molar flow between two elements A and B. As the binary diffusion constant at the molecular level is a known quantity, it follows at the mass level:

$$h_m = \frac{-D_{AB}\frac{\partial\rho_A}{\partial y}\Big|_{y=0\to\delta_t}}{\rho_{A,s}-\rho_{A,\infty}} \quad \text{(eq. 18)}$$

Hereafter, the convection mass transfer coefficient and the convection coefficient are proportional to the Lewis number Le, which measures the thermal diffusivity towards the mass diffusivity. Therefore, by imposing thermodynamic equilibrium, even in the absence or negligible mass transfer between the ullage and the molten salts, it follows the convection coefficient:

$$h = h_m\rho c_p Le^{1-n} \quad \text{(eq. 19)}$$

where:

$$Le = \frac{\alpha}{D_{AB}} \to Le^n = \left(\frac{\alpha}{D_{AB}}\right)^n = \frac{\delta_t}{\delta_c} \quad \text{(eq. 20)}$$

That is, the Lewis number to the n-th power is equal to the ratio between the temperature boundary thickness and the mass concentration boundary thickness. Although it is easy to verify that Le>>1, which means that the fluid transfers more heat than mass, *n* must be calculated accordingly, using a target value of:

$$n = log_{Le}\left(\frac{\delta_t}{\delta_c}\right) \approx \frac{1}{3} \to \sqrt[n]{\frac{\delta_t}{\delta_c}} = Le \quad \text{(eq. 21)}$$

$$\frac{h}{h_m} = \rho c Le^{1-n}, \qquad \frac{\delta_t}{\delta_c} = Le^n \;\Big|\; \frac{\delta_t}{\delta_c} : n \approx \frac{1}{3} \pm \varepsilon \quad \text{(eq. 22)}$$

Where the unknown *h* is found according to the convergence condition set to the side (eq. 21) and (eq. 22). By applying a trial-and-error method, knowing the value to which *n* must tend by 1/3, it obtains the convection coefficient *h*, namely a physical correlation between the molten salt and the ullage.

Secondly, based on this, the next step involves defining the actual boundary conditions of the Navier-Stokes equations in relation to the Fourier postulate and its corresponding equation. With respect to the Fourier postulate and its associated equation, as previously mentioned, in the thermodynamic equilibrium scenario of the Navier-Stokes equations, it is possible to approximate the internal energy *U* to that of a solid state for the

mass of salts, displaying natural temperature decay. In such extension, at certain stage it can be written:

$$\rho \frac{\partial U}{\partial \tau} = -\nabla \cdot (-k \nabla T) + \frac{\dot{E}_g}{dxdydz} \approx \rho c_p \frac{\partial T}{\partial \tau} \quad \text{(eq. 23)}$$

This equation is valid if and only if it is possible to write the variation in internal energy U as in a solid state and solely dependent on the specific heat regardless of whether at constant volume or pressure, and under the conditions that an infinite gradient of thermal perturbations can be accepted. And this indeed occurs when considering the propagation velocity to be essentially infinite at the point defining the thermal boundary layer.

Thirdly, to define the Navier-Stokes equations according to the contextual boundary conditions, the Knudsen number was calculated. For values of Kn≪0.01 the fluid dynamic motion is of the viscous type, given the value of the Boltzmann constant equal to $1.380649*10^{-23}$ J K^{-1}, T the operating temperature of the system, σ diameter of the NaNO3+KNO3, p the operating pressures of the system, and finally L as the characteristic free length of a particle. The average value found is equal to 0.0046 and therefore substantially viscous. In this regard, other studies (S. Sau et al., 2013; Bradshaw and Carling, 1987) show that the so-called Stokes assumption on viscosity can be applied, i.e. that the bulk viscosity for molten salts at the reference operating temperatures is zero. This implies a Newtonian fluid, viscosity independent on shear stress, and incompressibility of the salts, in particular, the viscous part of the Stokes differential equation transforms into:

$$\hat{d} = -\frac{2}{3}\mu \frac{\partial u_s}{\partial x_s} \hat{I} \quad \text{(eq. 24)}$$

Fourthly, the volume of the salts can be considered constant under the indicated conditions of validity, which implies that it is in an isochoric condition; it follows that the density must also be constant. Experimentally, it is verified that the non-variation of the density, under conditions of atmospheric pressure and in any case strictly less than $1.5*10^5$ Pa, leads to a maximum variation of the error between 6% and 9% according to 20 years gathered data. This assumption reduces unnecessary complexity of the calculation, but above all it leads and indicates that the variation of density with respect to pressure is zero, that is, the fluid does not depend on compression or stresses, hence the condition of incompressibility. This results in a certain simplification of the first Navier-Stokes equation (eq. 7) into:

$$\frac{\partial \rho}{\partial \tau} + \nabla \cdot \rho \tilde{u} = 0 \implies \nabla \cdot \tilde{u} = 0 \quad \text{(eq. 25)}$$

This has an important physical significance, namely that density transport is driven by the velocity vector. Typical phenomena are oceanographic currents, or parallel and stratified currents, as is well known for molten salts. This implies that the height above the reservoir is crucial for understanding the extent of heat transport and, consequently, the thermal phase lag of the different salt layers.

In summary, the equations (eq. 7), (eq. 8) and (eq. 9) are reduced to:

$$\nabla \cdot \tilde{u} = 0 \quad \text{(eq. 26)}$$

$$\rho \frac{\partial \tilde{u}}{\partial \tau} + \rho \nabla \tilde{u} \otimes \tilde{u} = \nabla \cdot \hat{d} \quad \text{(eq. 27)}$$

$$\rho \frac{\partial e}{\partial \tau} + \rho \nabla \cdot (e\tilde{u}) = -p \nabla \tilde{u} + \nabla \cdot (k \nabla T) + \hat{d} \nabla \tilde{u} \quad \text{(eq. 28)}$$

For the material derivative, up to the constant density it is comparable to the differential equations of entropy, enthalpy and temperature, that is:

$$\rho \frac{De}{D\tau} + p \nabla \tilde{u} = \nabla \cdot (k \nabla T) + \hat{d} \nabla \tilde{u} = \rho T \frac{Ds}{D\tau} = \rho \frac{Dh}{D\tau} = \rho c_p \frac{DT}{D\tau} \quad \text{(eq. 29)}$$

Fifthly, the conditions that define the temperature trend in the ullage are different which has a much lower thermal inertia and releases heat more quickly while maintaining low conductivity. When the immersed electrical resistors or the molten salt added to the boiler after energy capture are switched off, both the air and molten salt mediums begin to decay naturally. While the air immediately follows the laws of conduction transient, the salts retain energy for a certain period, which it has referred to as the inertial phase lag or displacement. Starting from the generic Navier Stokes equations for ullage, non-stationary, specific heat in the constant temperature range, negligible conductivity according to the Nusselt number, viscous flow (Kn=0), constant pressure, compressible and Newtonian fluid, it applies from general equations (eq. 7), (eq. 8) and (eq.

9) to ones of the ullage in terms of components as:

$$\frac{\partial \rho}{\partial \tau} + \frac{\partial \rho u_i}{\partial x_i} = 0 \qquad \text{(eq. 30)}$$

$$\frac{\partial \rho u_i}{\partial \tau} + \frac{\partial \rho u_i u_j}{\partial x_i} = \rho g_i - \frac{\partial}{\partial x_i}\left(\frac{2}{3}\mu \frac{\partial u_s}{\partial x_s}\right) \qquad \text{(eq. 31)}$$

$$c_p \frac{\partial \rho T}{\partial \tau} + c_p \frac{\partial \rho T u_i}{\partial x_i} = -p \frac{\partial u_i}{\partial x_i} - \frac{2}{3}\mu \frac{\partial u_s}{\partial x_s}\frac{\partial u_i}{\partial x_i} \qquad \text{(eq. 32)}$$

Finally, the last boundary condition is the application of GRGM for a function to be maximized with respect to the 0.057%÷0.1% of the maximum assumable value subject to the constraints that is aligned with the most probable value on the physical plane. This method can also lead to a non-convergent solution if the chosen initial value is too large for the wall conditions. It is observed that for initial values close to 0.40 meters or less the function converges. Furthermore, the wall law is solved in the same way with GRGM by setting small initial values of the function for δ and finding the convergence as a function of u^+ given the fluid dynamic coefficient B=0, since the state conditions for the temperature decay approximates a solid state.

5. Lumped- circuit

A certain similarity with complex first-order RL-RC electric circuits with complex time dynamics has been observed and used due to the presence of an element that stores energy in analogy to an inductor and/or capacitor. They differ in the way current and voltage vary over time in response to a change of state, such as the closing of a switch, due to the dynamic response properties, in perfect analogy to what was found in the analysis of the behaviour of the tank. Namely, specifically the expression characterized by (Angelillo et al., 2021; Turchetti et al., 2022; Angelillo et al., 2023):

$$\theta = \theta_i e^{-b\tau} + \tau^{log_\tau \theta^*}, \;\; log_\tau \theta^* = \frac{ln[\dot{Q}_0(\theta,\tau)=g]}{ln\,\tau} \qquad \text{(eq. 33)}$$

Where *de facto*:

$$\begin{matrix} \theta_i e^{-b\tau} \Rightarrow RC \\ \left(\frac{a}{b}\dot{P}(\theta,\tau) \Longrightarrow \tau^{log_\tau \theta^*}\right) \Rightarrow RL \end{matrix} \qquad \text{(eq. 34)}$$

The second part of the equation can be compared to a further complexity, that of the junction diode. As matter of fact, the junction diode is the one that best lends itself to the similarity of an inflection from one condition to another to emulate the end of the thermal phase shift as a collapse of the conditions of the wall which at a certain potential value changes its operation. The collapse of the inertial conditions is represented by finding the thermal boundary limit and therefore knowing the inertial thermal phase lag of molten salt φ, it can be imposed the necessary value for n in the Lewis number and through the GRGM represent the wall effect in a lumped circuit with a junction diode.

Returning to the general decay law (eq. 6) according to transient conduction, using the notations that above-lined-value indicates the geometric or mathematical mean of the value, an underlined-value indicates the value taken as constant, and above-and-underlined-value is the constant geometric or arithmetic mean of the values, it can be characterized as:

$$T_\tau = \left(\underline{T_0} - \underline{\overline{T_\infty}}\right) e^{b\tau} + \underline{\overline{T_\infty}} \qquad \text{(eq. 35)}$$

Where h in b is such that:

$$h: h = c_h \Delta h + \underline{\overline{h_0}} \qquad \text{(eq. 36)}$$

given that:

$$c_h = e^{\left(\frac{\delta_t}{\delta_c}\right)\frac{\tau}{\sum \tau}} \qquad \text{(eq. 37)}$$

Where the sum term represents the observation period of the closed tank system in which it shall be calculated the convection coefficient h, while the value Δh coincides with the internal value of the ullage. That is, according to the equation (eq. 19), (eq. 20), (eq. 21) and (eq. 22):

$$\Delta h = \bar{h}_i - \bar{h}_e = \bar{h}_i = \overline{\underline{h_0}} \equiv h = h_m \rho c_p L e^{1-n} \qquad \text{(eq. 38)}$$

In fact, when the exponential value is 0, it falls back into the conditions of the conduction transient, by contrast, a different value when it reaches a threshold according to the wall conditions indicated so far. Hence, writing the relationship:

$$h = \overline{\underline{h_0}} \left(e^{\left(\frac{\delta_t}{\delta_c}\right)\frac{\tau}{\Sigma\tau}} - 1 \right) \qquad \text{(eq. 39)}$$

with a clear similarity to those of an ideal Shockley junction diode. Once adapted to the lumped circuit, it can work in OpenModelica simulation properly.

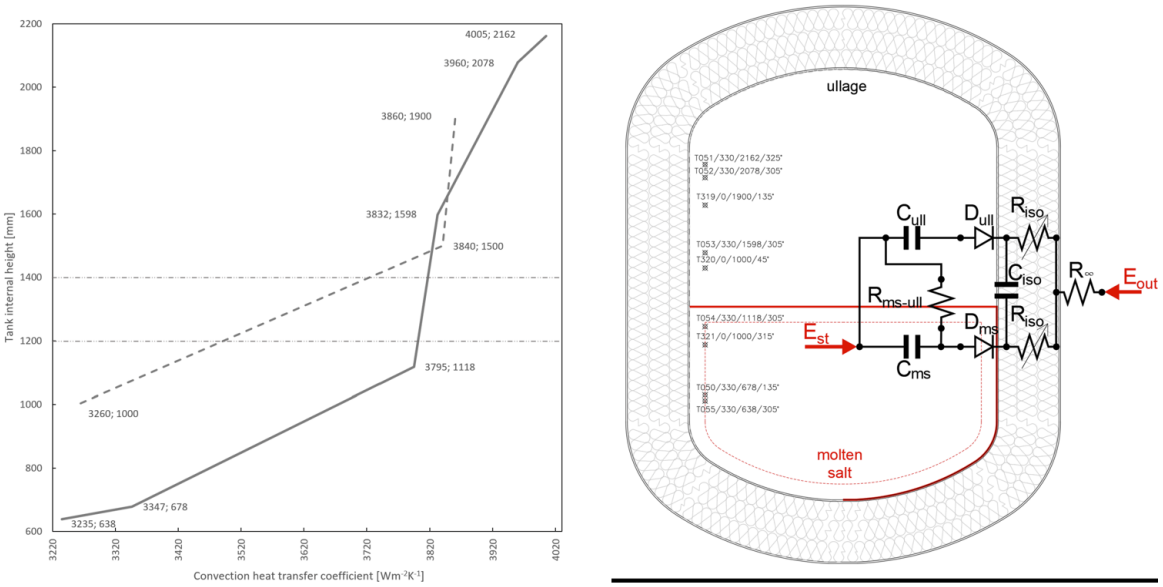

Figure 5 On the left the relationship between the found values of the convection heat transfer coefficient and the height of the tank. On the right the position and data of thermocouples [Name of thermocouples/distance from the shell/Height from the bottom/Angle with respect to the north 0°] plus the lumped circuit with new junction-diodes components.

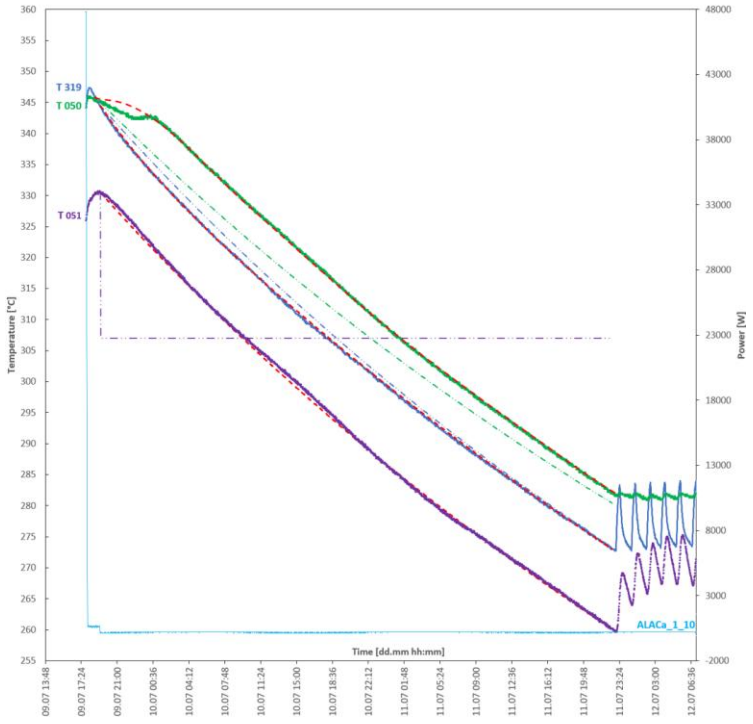

Figure 6 Real data each 5 sec. between 9.7.2004 and 12.07.2004 of thermocouples T050-molten salts, T051-ullage, T321-tank-skin. The red dotted lines are the respective results of the presented model. The coloured long-dash-dot-dot lines are the same results applying the approach by literature. No external thermal power input, during decay.

6. Results, discussion, conclusions and outlook

The analytical solution is based on the research of the control parameters necessary to identify the thermal displacement conditions, and among others the heat transfer coefficient, reformulated as a junction-diode. As a matter of fact, Figure 5 shows how the sudden jump of this value read on the tank shell undergoes in total analogy to a diode and to skin effect electromagnetic phenomena. In particular, the possibility of using the Lewis number is a novelty for the scope to find the value of the initial heat transfer coefficient, assuming that for Le>>1 more heat than mass is naturally transferred between air and molten salts, see (eq. 19), (eq. 20), (eq. 21), (eq. 22), (eq. 38) and (eq. 39) when it may concerns OpenModelica simulation.

In order to give physical meaning to the implementation of the temperature decay formulation where the choice of the initial temperature is fundamental, the whole fluid dynamic model has been discretised for a OpenFoam simulation in a forthcoming publication. Assuming that the variation of the heat transfer coefficient was linked to both the speed and the diffusion of heat, both considered equal in the two Cartesian directions for the ullage and negligible for the molten salts due to the peculiarity of the latter to stratify, the initial velocity can be taken as proportion between the variation of time, temperature and convection over viscosity. Ergo, given all the equations for density, conductivity, diffusivity, specific heat, dynamic and kinetic viscosity, into a domain of the neighbouring values in a split grid, the variations on the model should be compelled in a neighbourhood equal to ΔT=0,000329 K, and Δh=1,33 $Wm^{-2}K^{-1}$, to obtain a Courant number (Courant et al.,1927) close to stability and accuracy in a simulation. Since the flow regimes are viscous and incompressible-wise, but not Newtonian as at whole, the boundary conditions for the Navier-Stokes equations are based on the idealized Generalized Newtonian fluid model (Kn<0.01). Indeed, the study provided by S. Sau et al. (2013) has demonstrated and supports that $NaNO_3$+KNO_3 60/40 can be a Newtonian fluid. Furthermore, assuming that the tank is at atmospheric pressure, or nevertheless less than $1.5*10^5$ Pa with substantially irrelevant variations caused by it, the reference equations for the control volumes are (Eq. 2), (Eq. 3), (Eq. 6), (Eq. 15), (Eq. 16), (Eq. 17), (Eq. 19), (Eq. 23), (Eq. 26), (Eq. 27), (Eq. 28), (Eq. 29), (Eq. 30), (Eq. 31), (Eq. 32) and (Eq. 39).

Namely, Figure 6 shows the results of the new model compared to the general formulations of natural decay of temperature given the fundamental physical characteristics of the observed materials. Ceteris paribus, in the figure the red dotted lines are the results of the presented model, namely a quasi-perfect match with the real measured data, while the coloured long-dash-dot-dot lines per thermocouples are the results applying the transient conduction. The thermocouple T051 represents measurements made in the ullage, the curve T050 are the measurements of a thermocouple immersed in the molten salts, while T319 are the measurements on the tank shell.

To conclude, the objective of this work was to analyse natural decay in detail to predict further the performance of energy storage tanks over a sufficiently reliable timeframe. Significant differences were observed between the new model and transient conduction approaches found in the literature acknowledge the molten salt thermal displacement. Consistent results can allow for year-to-year comparisons to evaluate tank performance and predict-plan thermal insulation maintenance monitoring aging. Besides, this study can aid to identify the maximum usage time of the hottest molten salt core, both during an off-design and a new tank project, improving storage, conducting in-depth/sensitive studies on tank parameters, implementing internal heat exchangers as overall system performance. These are the subject of forthcoming publications.

7. Acknowledgments

The authors acknowledge ENEA for the scientific and technical support provided during the experimental campaigns SURPF2001170003A and SURPF2201170005 to PCS facility. The access SURPF2001170003A was arranged in the frame of H2020 SFERA-III project activities – European Union's Horizon 2020 G.A. n.823802 –.

8. References

Afrah Awad, Helena Navarro, Yulong Ding, Dongsheng Wen, 2018, Thermal-physical properties of nanoparticle-seeded nitrate molten salts, Renewable Energy, 120, 275-288

Anagnostopoulos A., Alexiadis A., Ding Y., 2019, Molecular dynamics simulation of solar salt (NaNO3-

KNO3) mixtures, Solar Energy Materials and Solar Cells, Volume 200, 1099897

Angelillo A., Gaggioli W., Di Ascenzi P., 2021 Boundary conditions and Natural temperature decay from experimental data analysis to on-design of a tank for CSP plant - Part 1, International Solar Energy Society Conference Proceedings Solar World Congress 2021 Virtual Conference

Angelillo A., Gaggioli W., Di Ascenzi P., Boundary conditions and Natural temperature decay from experimental data analysis to on-design of a tank for CSP plant - Part 2, International Solar Energy Society Conference Proceedings Solar World Congress 2023 New Delhi

Bergman T.L., Lavine A.S., 2017. Fundamentals of heat and mass transfer. 8th ed. Wiley, USA.

Bonk A., Bauer T., 2021, Solar Salt – Thermal Property Analysis, Scientific Report: DLR-FB-2021-19

Bradshaw R. W., Carling R. W., 1987, A review of the chemical and physical properties of molten alkali nitrate salts and their effect on materials used for solar central receivers, ECS Proceedings, Vol. 1987-7 959

Chaudhuri N., Feireisl E., 2022. Navier–Stokes–Fourier system with Dirichlet boundary conditions, Applicable Analysis, 101:12, 4076-4094.

Cornwell K., 1970, The thermal conductivity of molten salts, Department of Mechanical Engineering, Edinburgh

Courant R., Friedrichs K., Lewy H., 1927. On the partial difference equations of mathematical physics. IBM journal Math.

DiGiulio R. M., Teja A. S., 1992, The Thermal Conductivity of the Molten NaNO3-KNO3 Eutectic Between 525 and 590 K, International Journal of Thermophysics, Vol. 13, No. 4

Janz G.J., Allen C.B., Bansal N.P., Murphy R.M., Tomkins R.P.T., 1979, Physical Properties Data Compilations Relevant to Energy Storage, NSRDS-NBS 61, Part II

Janz G.J., Bansai N.P., 1982. Molten Salts Data: Diffusion Coefficients in Single and Multi-Component Salt Systems. Journal of Physical and Chemical Reference Data, vol.11, nr.3.

Janz G.J., Dampier F.W., Lakshminarayanan G.R., Lorenz P.K., Tomkins R.P.T., 1968. Molten salts: Volume 1, Electrical Conductance, Density, and Viscosity Data. NSRDS-National Standard Reference Data Series-.

Milozzi G.M., Giannuzzi, P. Tarquini, A. La Barbera, 2001, Fluido termovettore: dati di base della miscela di nitrati di sodio e potassio, s.l. – Doc.ENEA/SOL/RS/2001/07

Nunes V.M.B., Queirós C.S., Lourenço M.J.V., Santos F.J.V., Nieto de Castro C.A., 2016, Molten salts as engineering fluids – A review Part I. Molten alkali nitrates, Applied Energy, 183, 603-611

Qing-Guo Zhao, Chun-Xu Hu, Su-Jie Liu, Hang Guo, Yu-Ting Wu, 2017, The Therma conductivity of molten salt NaNO3, KNO3, and their mixtures, Energy Procedia, 143, 774-779

Saivenkataraman Jayaraman, Aidan P. Thompson, O. Anatole von Lilienfeld, Edward J. Maginn, 2010, Molecular Simulation of the Thermal and Transport Properties of Three Alkali Nitrate Salts, Industrial & Engineering Chemistry Research, 49, 559-571

Sau S., Veca E., Corsaro N., 2013, Nitrati fusi come fluido termovettore intermedio. Confronto fra miscela binaria ed una ternaria contenente calcio, ENEA Report RdS/2013/019, 2013

Turchetti L., Di Ascenzi P., Petroni G., Angelillo A., Gaggioli W., 2022, Experimental investigation of a freezing-thawing cycle in a molten salt storage tank, 28th SolarPACES Conference Albuquerque NM USA

Zavoico A.B., 2001, Solar power tower design basis document. Sandia National Laboratories. Report no. SAND2001-2100

Ze Sun, Lei Su, Xianyang Gao, Guimin Lu, Xingfu Song, Jianguo Yu, 2021, Influences of impurity Cl- on the thermal performance of solar salt for thermal energy storage, Solar Energy 216, 90–95

Zhang X., Fujii M., 2000, Simultaneous Measurements of the Thermal Conductivity and Thermal Diffusivity of Molten Salts with a Transient Short-Hot-Wire Method, International Journal of Thermophysics, Vol. 21/1